0026-895X/94/061168-07$03.00/0

MOLECULAR PHARMACOLOGY, 46:1168–1174, 1994.

Unusual Pharmacology of (+)-Tubocurarine with Rat Neuronal Nicotinic Acetylcholine Receptors Containing β4 Subunits

ARMAND B. CACHELIN and GABRIELE RUST
Department of Pharmacology, University of Berne, 3010 Bern, Switzerland
Received June 22, 1994; Accepted September 26, 1994

SUMMARY

We have investigated the functional properties of four rat neuronal nicotinic acetylcholine receptor types expressed in *Xenopus* oocytes after injection of pairwise combinations of mRNA encoding α2 or α3 receptor subunits with mRNA encoding β2 or β4 receptor subunits. Current responses evoked by rapid application of cholinergic agonists (acetylcholine, nicotine, or 1,1-dimethyl-4-phenylpiperazinium) were recorded from voltage-clamped oocytes. Substituting $BaCl_2$ for $CaCl_2$ in the external solution increased the apparent K_d values of β4 subunit-containing receptors for acetylcholine but decreased the apparent K_d values of β2 subunit-containing receptors. Inhibition curves for the cholinergic antagonist (+)-tubocurarine were measured in $BaCl_2$ medium at low agonist concentrations. (+)-Tubocurarine was a competitive antagonist of acetylcholine at neuronal nicotinic acetylcholine receptors that coexpressed the β2 subunit; the estimated K_b values were 3.6 μM (α2β2 receptors) and 390 nM (α3β2 receptors). In contrast, (+)-tubocurarine enhanced the peak responses evoked by low acetylcholine concentrations at α2β4 and α3β4 neuronal nicotinic acetylcholine receptors, without being a partial agonist. The maximal increase was observed at 5 μM and 10 μM (+)-tubocurarine for α2β4 and α3β4 receptors, respectively. Higher (+)-tubocurarine concentrations inhibited cholinergic responses, thus yielding a "bell-shaped" concentration-response curve.

nAChRs belong to a superfamily of membrane proteins that transmit fast synaptic signals. These ligand-activated receptors share a common assembly principle, consisting of a pseudosymmetric arrangement of five membrane-spanning subunits surrounding an ion-conducting channel. nAChRs mediate fast excitatory signal transduction at the neuromuscular junction (muscle type) and at interneuronal synapses in the central and autonomic nervous system (neuronal type). Muscle-type nAChRs consist of four subunits with a stoichiometry of $\alpha_2\beta\gamma\delta$ or $\alpha_2\beta\epsilon\delta$. In contrast, neuronal nAChRs appear to consist of only agonist-binding (α) and nonbinding (non-α or β) subunits (for reviews, see Refs. 1 and 2). Thus far, 10 different cDNAs encoding subunits of the neuronal nAChR (α2-α8 and β2-β4) have been cloned from rat, chick, and other neuronal tissues (for reviews, see Refs. 3 and 4). Functional neuronal nAChRs have been expressed in *Xenopus* oocytes after injection of mRNA encoding a single α subunit (α7) or various combinations of mRNAs encoding α and β subunits (for reviews, see Refs. 5 and 6). Recent studies suggest, however, that the subunit composition of certain neuronal nAChRs expressed *in vivo* may be more complex, including two different α subunit isoforms within the same receptor type (7–9).

The pharmacology and kinetic properties of neuronal nAChRs differ from those of endplate receptors (10). Studies of the functional properties of neuronal nAChRs of known subunit composition have begun to shed some light on the relation between structure and function of these receptors. Neuronal bungarotoxin, for example, selectively blocks α3β2 neuronal nAChRs but barely affects agonist-evoked responses with other neuronal or endplate nAChRs (3, 11). α-Bungarotoxin blocks only homomeric α7 nAChRs or hetero-oligomeric α7α8 nAChRs (for review, see Ref. 12). The subunit composition of neuronal nAChRs also determines their pharmacological (13–15) and kinetic properties, such as time course of desensitization (16, 17), channel mean open time (18), and calcium permeability (19, 20).

(+)-Tubocurarine has a broad range of pharmacological properties. It is a competitive antagonist of ACh at end-plate nAChRs (21), at neuronal nAChRs of frog cardiac and paravertebral neurons (22), and at chick α4/non-α receptors expressed in *Xenopus* oocytes (23). On the other hand, it is also a partial agonist at muscle nAChRs (Refs. 24 and 25 and references cited therein) and at neuronal nAChRs of bovine chromaffin cells (26).

The aim of this study was to determine whether the unusually varied pharmacology of (+)-tubocurarine is linked to specific neuronal nAChR types. We show here that (+)-tubocurarine

This work was supported by Swiss National Science Foundation Grant 31.31018.91, The Roche Research Foundation, The Sandoz Foundation, and the Hochschulstiftung (to A.B.C.).

ABBREVIATIONS: nAChR, nicotinic acetylcholine receptor; ACh, acetylcholine; DMPP, 1,1-dimethyl-4-phenylpiperazinium; HEPES, 4-(2-hydroxyethyl)-1-piperazineethanesulfonic acid.

inhibits the ACh-evoked responses of $\alpha2\beta2$ and $\alpha3\beta2$ neuronal nAChRs in a concentration-dependent manner. The concentration-response curves obtained for $\alpha2\beta4$ and $\alpha3\beta4$ nAChRs were bell-shaped, suggesting a dual effect of (+)-tubocurarine on these receptor types. With $\alpha2\beta4$ and $\alpha3\beta4$ receptors, the inhibition of the responses is likely to result from competitive and noncompetitive antagonism (open channel block).

Materials and Methods

mRNA preparation. cDNA clones encoding rat neuronal nAChR subunits ($\alpha2$, $\alpha3$, $\beta2$, and $\beta4$) were gifts from Drs. J. Boulter and S. Heinemann (The Salk Institute, La Jolla, CA) and Dr. J. Patrick (Baylor College, Houston, TX). Capped mRNAs were prepared using *in vitro* transcription with T3 or T7 polymerase, in the presence of the 5′ cap analog 5′-7-methyl-GpppG (27). mRNAs were tailed with poly(A)$^+$ using poly(A)$^+$ polymerase (Boehringer), according to standard methods (28). Aliquots containing about 200 ng of capped and poly(A)$^+$-tailed mRNA were stored at −20° C until used. mRNAs were pelleted and resuspended in 5 mM HEPES solution, pH 7.4, for injection. *Xenopus* oocytes (stage V or VI) (29) were injected with pairwise combinations of α and β subunit mRNAs, at a final concentration of approximately 160 ng of mRNA/μl (50 nl/oocyte).

Signal recording. Denuded oocytes (30) were used 4–12 days after mRNA injection. Agonist-evoked responses were measured in voltage-clamped oocytes (holding potential, −80 mV) by using a two-electrode voltage-clamp amplifier (Axoclamp 2A; Axon Instruments, Foster City, CA). Current and voltage signals were digitized on-line (VR10A; Instrutech Corp., Elmont, NY) and stored on video tape. Experiments were later played back, filtered (f_c = 10 or 50 Hz, −3 db, Bessel filter), and resampled at 10 or 50 Hz (CHART program, version 2; Cambridge Electronic Design, Cambridge, UK), using a microcomputer and a programmable analog/digital converter (CED 1401; CED). Data analysis, curve fitting (Marquardt-Levenberg method), and plotting were done on a Macintosh microcomputer using Kaleidagraph (version 3.0; Synergy Software, Reading, PA).

Solutions. Experiments were performed in external solution ($CaCl_2$ medium) containing 90 mM NaCl, 1 mM KCl, 1 mM $MgCl_2$, 1 mM $CaCl_2$, and 5 mM Na-HEPES (pH adjusted to 7.4 with NaOH). The activation of Ca^{2+}-activated Cl^- channels during activation of nAChRs (31) was minimized by using nominally calcium-free external solution in which $CaCl_2$ was replaced by $BaCl_2$ ($BaCl_2$ medium). The Ca^{2+} concentration of this solution, determined by atomic absorption spectrophotometry (model 353; Instrumentation Laboratory), was <5 μM. Frozen aliquots of ACh chloride (Sigma), DMPP iodide (Fluka), (−)-nicotine di-(+)-tartrate (Sigma), and (+)-tubocurarine chloride (Sigma) stock solutions were diluted in external solution to the required final concentrations. Rapid exchange of solutions was achieved by applying solutions through a narrow glass tube (diameter, ≈1.5 mm) placed above the equator of the oocyte and directed at the animal pole of the oocyte.

Curve fitting and parameter estimation. Concentration-response curves were fitted with the Hill equation,

$$I_{(x)} = I_{max}\frac{C_A{}^n{}_H}{1 + C_A{}^n{}_H} \quad (1)$$

where I_{max} is the maximal response, n is the Hill coefficient, and c_A is the normalized agonist concentration (x/K_a). Estimates of IC_{50}, the antagonist concentration that causes 50% reduction of a control response, were obtained by fitting the following equation to the normalized data points:

$$I_{(x)} = 100\left(1 - \frac{x^n{}_H}{x^n{}_H + IC_{50}{}^n{}_H}\right) \quad (2)$$

where I_x is the current response and x is the antagonist concentration. Estimates of K_b, the affinity of the antagonist, were obtained by applying the 'functional equivalent' of the Cheng-Prusoff relation (32). Thus,

$$K_b = \frac{IC_{50}}{1 + c_A} \quad (3)$$

where c_A is the normalized agonist concentration, as defined above.

Agonist-induced activation of the nAChR was assumed to follow consecutive binding of two ACh molecules, thus yielding a three-state kinetic scheme, as previously used for the end-plate nAChR (31). A six-state kinetic scheme simplified from the original scheme (33) by omitting an additional isomerization step after binding of two agonist molecules was used to model responses obtained in the presence of agonist and (+)-tubocurarine.

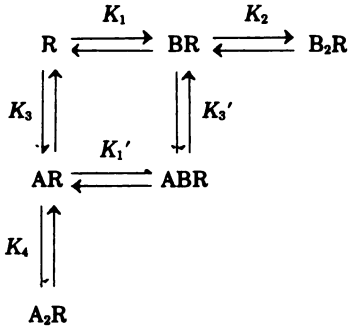

We assumed, for the sake of simplicity, that binding of agonist or antagonist molecule to either binding site was independent of the occupancy state of the other binding site, thus yielding the following constraints: $K_1 = K_2$, $K_3 = K_4$, and finally $K_1' = K_1$ (for the antagonist) and $K_3' = K_3$ (for the agonist) (where K_n is the equilibrium dissociation constant of the n^{th} step). According to this scheme the occupancy of the open state, p_{open}, in the presence of agonist and competitive antagonist is equal to

$$P_{open} = \frac{c_A{}^2}{(1 + c_A + c_B)^2} \quad (4)$$

where c_A is the normalized agonist concentration and c_B is the normalized antagonist concentration x_B/K_b. To obtain a bell-shaped concentration-response curves, we assumed that the intermediate ACh- and (+)-tubocurarine-liganded state was conducting. The total current response is then a function of the sum of the occupancies of the open state and of this intermediate state,

$$I_{x_Ax_B} = I_{max}\frac{c_A{}^2 + 2fc_Ac_B}{(1 + c_A + c_B)^2} \quad (5)$$

where f is an arbitrary factor describing the ratio of the average current through the intermediate state with respect to the current through the normal open state ($I_{avg} = Npi$, where N is the number of channels, p is the open probability, and i is the single-channel current), and I_{max} is the ratio between maximal current response and current elicited by c_A (i.e., $1/p_{open}$). I_{max} was a free parameter for curve-fitting procedures.

Results

Concentration-Response Curves

The apparent K_d for each receptor type was determined in a first set of experiments. We then used the single-point method (inhibition curves) to determine the K_b of (+)-tubocurarine, as explained in Materials and Methods.

Current responses were measured in *Xenopus* oocytes expressing neuronal nAChRs after injection of $\alpha2/\beta2$, $\alpha2/\beta4$, $\alpha3/\beta2$, or $\alpha3/\beta4$ subunit-encoding mRNAs. Most results were obtained in nominally calcium-free external solution, in which

$CaCl_2$ was replaced by $BaCl_2$ to minimize activation of Ca^{2+}-dependent chloride currents. Additional results obtained in physiological $CaCl_2$ medium are shown for comparison.

Concentration-response curves in $BaCl_2$ medium. Current responses became detectable at submicromolar concentrations of ACh (200–500 nM) and reached maximum levels (6–9 μA) at concentrations above 200 μM. The peak responses increased in a concentration-dependent manner. We often observed a reduction of the peak responses at high agonist concentrations (>1 mM).

Data from several experiments were normalized and averaged before analysis. Half-logarithmic plots of the peak responses as a function of agonist concentration were sigmoidal for all four combinations (Fig. 1). Normalized and averaged data were pooled for analysis (see Materials and Methods). Each combination was characterized by a specific K_a; ACh was most potent at α3β2 nAChRs (24 μM), followed by α2β4 nAChRs (44 μM), α3β4 nAChRs (77 μM), and α2β2 nAChRs (87 μM). The slopes of the concentration-response curves showed some dependence on the β subunit. The Hill coefficients of the concentration-response curves for β2-containing nAChRs (α2β2, n_H = 1.0; α3β2, n_H = 0.8) were somewhat smaller than those of β4-containing nAChRs (α2β4 and α3β4, n_H = 1.2) (Table 1).

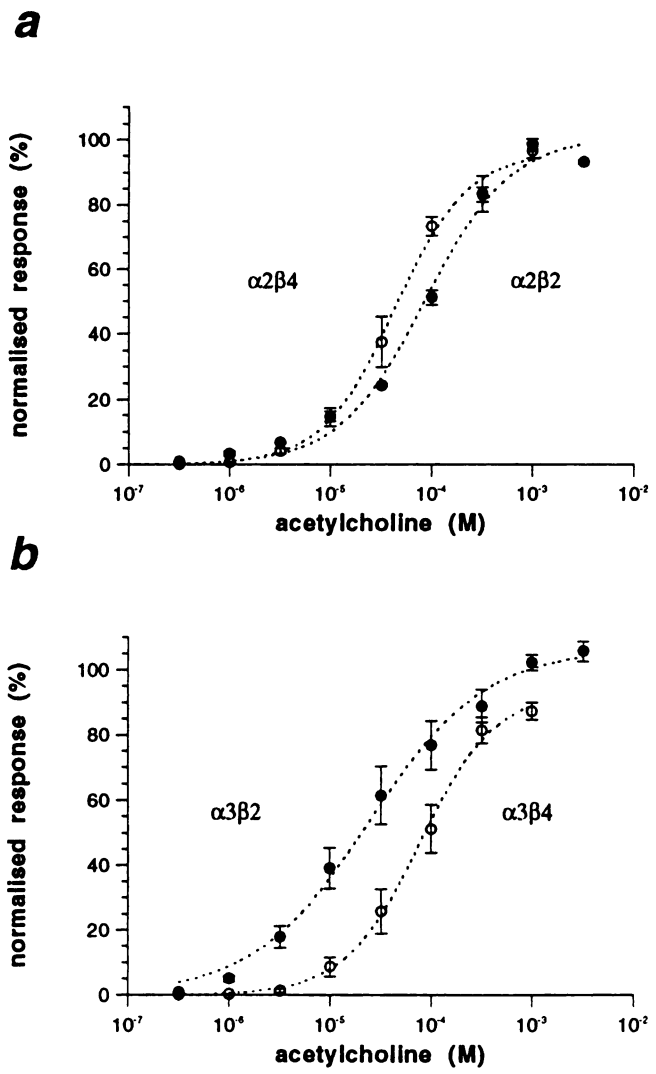

Fig. 1. Concentration-response curves for neuronal nAChRs in $BaCl_2$ medium. Data points were normalized with respect to the initially determined maximal response I_{max}. Apparent K_d (K_a) and Hill coefficient (n) values were obtained by fitting the Hill equation to the averaged data (see Materials and Methods). a, ●, α2β2 receptors; ○, α2β4 receptors; b, ●, α3β2 receptors; ○, α3β4 receptors (see Table 1 for parameters estimates).

Concentration-response curves in $CaCl_2$ medium

Each combination was characterized by its individual affinity for ACh. ACh was most potent at α2β4 nAChRs (19 μM), followed by α3β2 nAChRs (44 μM), α3β4 nAChRs (52 μM), and α2β2 nAChRs (155 μM). Thus, whereas the K_a estimates for β2-containing nAChRs were increased about 2-fold by the presence of Ca^{2+} (1 mM) in the external solution, those for β4-containing receptors were decreased in the same proportion. The slopes of the concentration-response curves were barely affected by the substitution of $CaCl_2$ for $BaCl_2$ in the external solution (α2β4 and α3β4, n_H = 1.2; α2β2 and α3β2, n_H = 1.1) (Table 1).

Effects of (+)-Tubocurarine

α2β2 and α3β2 neuronal nAChRs. Fig. 2 shows superimposed responses obtained when (+)-tubocurarine was applied at concentrations ranging from 15 nM to 50 μM together with 2 μM ACh, a concentration well below the estimated K_a for these receptor types. (+)-Tubocurarine caused a concentration-dependent decrease of the peak response without causing any visible increase in the rate of decay of the responses. High (+)-tubocurarine concentrations (15 and 50 μM) virtually abolished the ACh-evoked responses (Fig. 2).

Control responses evoked by application of the agonist alone were used to normalize subsequent responses. Inhibition curves were then constructed by pooling and averaging normalized data. Estimates of IC_{50}, the concentration required for half-maximal inhibition, were obtained using an empirical inhibition curve (eq. 2 and Fig. 3). The estimates of IC_{50} were 3.7 μM for α2β2 nAChRs and 420 nM for α3β2 nAChRs. The calculated K_b values were 3.6 μM (α2β2) and 390 nM (α3β2), with slopes close to 1 (Table 2). Similar K_b estimates and slopes were obtained in $CaCl_2$ medium (3.3 μM for α2β2 nAChRs and 630 nM for α3β2 nAChRs) (Table 2).

α2β4 and α3β4 neuronal nAChRs. (+)-Tubocurarine concentrations ranging from 50 nM to 150 μM were applied together with low ACh concentrations (α2β4, 2 μM; α3β4, 4 μM) in $BaCl_2$ medium, as described above. Fig. 4a shows superimposed responses obtained with α2β4 nAChRs. The peak current response was somewhat inhibited by low (+)-tubocurarine concentrations (<150 nM). Higher concentrations (up to 15 μM)

TABLE 1

Apparent equilibrium dissociation constants (K_a) and Hill coefficients (n_H) for ACh in neuronal nAChRs

Parameter estimates were obtained using the Hill equation to fit the normalized and averaged data of n concentration-response curves, as described in Materials and Methods (estimates ± error).

Subunit combination	$CaCl_2$ medium			$BaCl_2$ medium		
	K_a	n_H	n/ donors	K_a	n_H	n/ donors
	μM			μM		
α2β2	155 ± 24	1.1 ± 0.1	3/1	87 ± 15	1.0 ± 0.2	3/2
α3β2	44 ± 4.0	1.1 ± 0.04	4/1	24 ± 3.8	0.8 ± 0.1	6/3
α2β4	19 ± 1.1	1.2 ± 0.1	3/1	44 ± 4.7	1.2 ± 0.1	7/3
α3β4	52 ± 6.4	1.2 ± 0.1	3/1	77 ± 7.2	1.2 ± 0.1	7/3

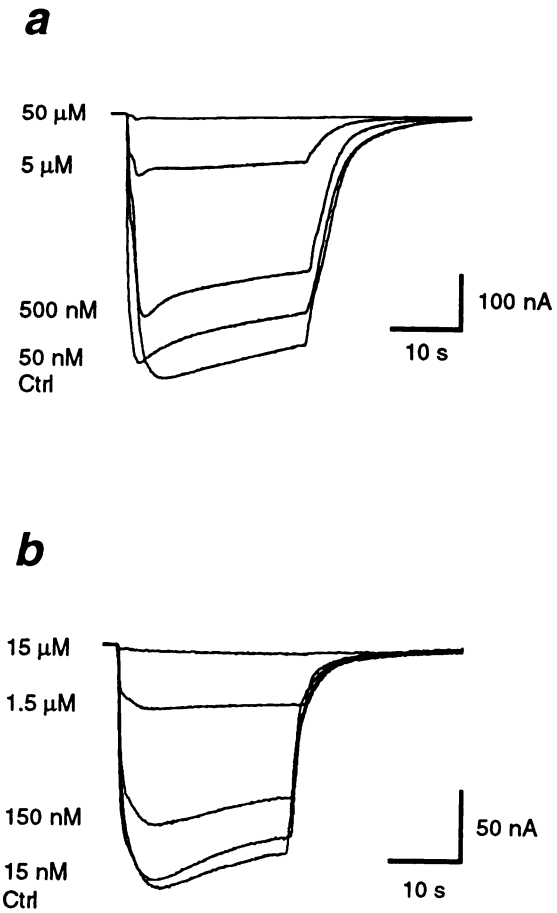

Fig. 2. Effect of (+)-tubocurarine on ACh-evoked responses with $\alpha2\beta2$ and $\alpha3\beta2$ neuronal nAChRs. Control responses (*Ctrl*) were elicited by application of 2 μM ACh in nominally calcium-free $BaCl_2$ medium. Gradual inhibition of the responses was obtained by simultaneous application of (+)-tubocurarine, at the indicated concentrations, together with 2 μM ACh. a, $\alpha2\beta2$ receptors; b, $\alpha3\beta2$ receptors. (Holding potential, −80 mV).

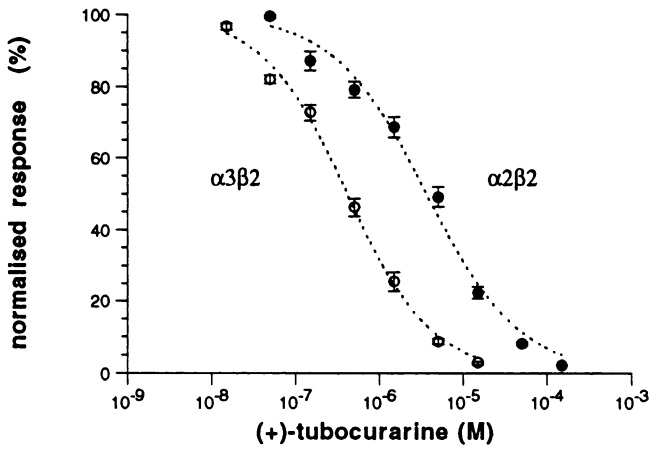

Fig. 3. Inhibition of $\alpha2\beta2$ and $\alpha3\beta2$ neuronal nAChRs by (+)-tubocurarine. Peak currents were normalized with respect to the individual peak currents elicited by 2 μM ACh in the absence of antagonist. Estimates of IC_{50} obtained by nonlinear regression of eq. 2 (see Materials and Methods) were 3.6 μM ($\alpha2\beta2$ receptors) (●) and 390 nM ($\alpha3\beta2$ receptors) (○). Each *point* is the mean ± standard error ($\alpha2\beta2$, $n = 7$ from three donors; $\alpha3\beta2$, $n = 4$) (Table 2).

TABLE 2

Affinity of (+)-tubocurarine for $\alpha2\beta2$ and $\alpha3\beta2$ neuronal nAChRs

Inhibition curves were obtained by applying various (+)-tubocurarine concentrations in the presence of 2 μM ACh (Figs. 2 and 3). Estimates of IC_{50} were obtained by fitting an inhibition curve to the data points, as described in Materials and Methods. Estimates of K_b were obtained as $K_b = IC_{50}/(1 + c_A)$, where c_A is the normalized agonist concentrration x/K_a. The estimates of K_a obtained under the same experimental conditions are taken from Table 1.

Subunit combination	IC_{50}	Slope	K_b	*n*/ donor(s)
	μM		μM	
$\alpha2\beta2$ ($BaCl_2$)	3.7 ± 0.5	0.8 ± 0.07	3.6	7/3
$\alpha3\beta2$ ($BaCl_2$)	0.42 ± 0.03	0.9 ± 0.05	0.39	4/1
$\alpha2\beta2$ ($CaCl_2$)	3.3 ± 0.3	1.1 ± 0.08	3.3	2/1
$\alpha3\beta2$ ($CaCl_2$)	0.63 ± 0.05	1.0 ± 0.07	0.60	5/3

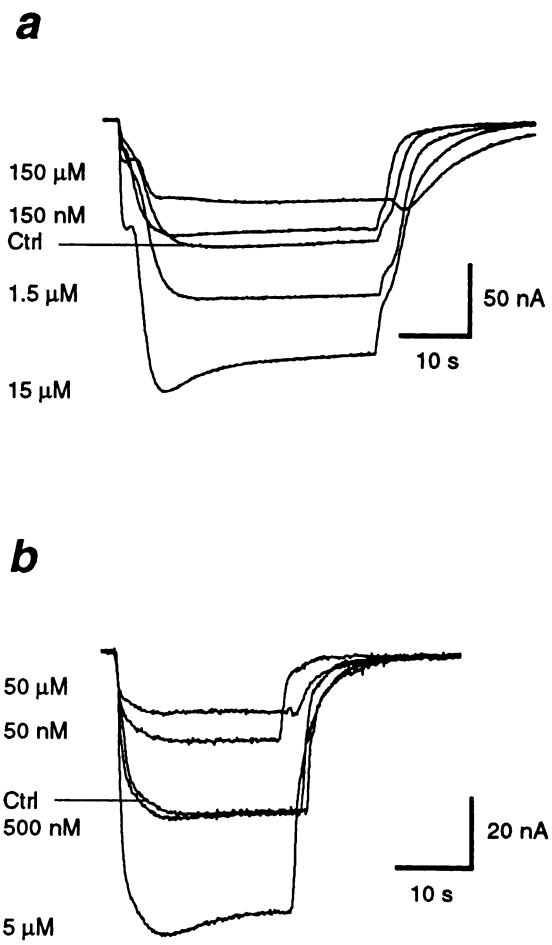

Fig. 4. Effect of (+)-tubocurarine on ACh-evoked responses with $\alpha2\beta4$ and $\alpha3\beta4$ neuronal nAChRs. Responses were elicited by bath application of ACh in nominally calcium-free $BaCl_2$ medium. The coapplied (+)-tubocurarine concentrations are indicated. a, $\alpha2\beta4$ receptors; responses elicited by 2 μM ACh. b, $\alpha3\beta4$ receptors; responses elicited by 4 μM ACh. *Ctrl*, control. (Holding potential, −80mV).

significantly increased the agonist-induced peak response (+115%) (Fig. 4). Application of still higher concentrations of antagonist inhibited the peak response, although coapplication of 150 μM (+)-tubocurarine did not completely inhibit the ACh-evoked response (Fig. 4a). We observed a similar response-enhancing effect of (+)-tubocurarine on responses evoked by 4 μM ACh with $\alpha3\beta4$ receptors. The inhibition of the response by low (+)-tubocurarine concentrations was more pronounced than with $\alpha2\beta4$ nAChRs. Also, the maximal enhancement of

the response was reached at somewhat lower (+)-tubocurarine concentrations [+88% with 5 μM (+)-tubocurarine] (Fig. 4b). Thus, the effect of (+)-tubocurarine on these two receptor types differed strikingly from its effect on the receptors expressed after injection of the corresponding α mRNA with β2 mRNA.

Data from α2β4 and α3β4 nAChRs were pooled and averaged for further analysis (Fig. 5). The average response-enhancing effect of (+)-tubocurarine was maximal between 5 and 15 μM with α2β4 nAChRs (65 ± 25%) and at 5 μM with α3β4 nAChRs (64 ± 14%). Application of 5, 50, or 150 μM (+)-tubocurarine alone to α2β4 or α3β4 nAChRs did not elicit any detectable response ($n \geq 5$ from two to four donors for either combination) (data not shown).

Responses of α3β4 nAChRs elicited by 30 μM (−)-nicotine in $CaCl_2$ medium were increased to 140 ± 16% by 5 μM (+)-tubocurarine ($n = 2$). In contrast, responses elicited by 5 μM DMPP were not enhanced by coapplication of 1.5 μM (+)-tubocurarine. We observed an average reduction of the peak responses to 68 ± 3.5% of the control response when 1.5 μM (+)-tubocurarine was applied with 5 μM DMPP ($n = 3$). However, in the same oocytes, coapplication of 1.5 μM (+)-tubocurarine with 20 μM ACh increased the agonist response.

Responses of α3β4 nAChRs evoked by 20 μM ACh in $CaCl_2$ medium were enhanced to 139 ± 12% by 1.5 μM (+)-tubocurarine ($n = 8$ from three donors). We also observed an enhancement of responses of α2β4 nAChRs to 2 μM ACh when 1.5 μM (+)-tubocurarine was coapplied in $CaCl_2$ medium (+63 ± 8%, $n = 3$).

In an additional set of experiments, we assessed the stimulatory effect of (+)-tubocurarine as a function of the agonist concentration in $BaCl_2$ medium (Fig. 6). The enhancement of the response of α2β4 nAChRs induced by 1.5 μM (+)-tubocurarine was maximal (about 95%) at ACh concentrations of ≤1 μM. Increasing the ACh concentration increased the absolute size of the response but markedly reduced the response enhancement induced by (+)-tubocurarine. (+)-Tubocurarine (1.5 μM) inhibited the responses to 10 and 32 μM ACh by 5% and 27%, respectively (Fig. 6).

ACh-evoked responses of a high proportion of β4 receptor-expressing oocytes from one donor (four of 11, 36%) were not enhanced by (+)-tubocurarine. The ACh-induced responses of all β4 receptor-expressing oocytes from five additional donors were enhanced by (+)-tubocurarine.

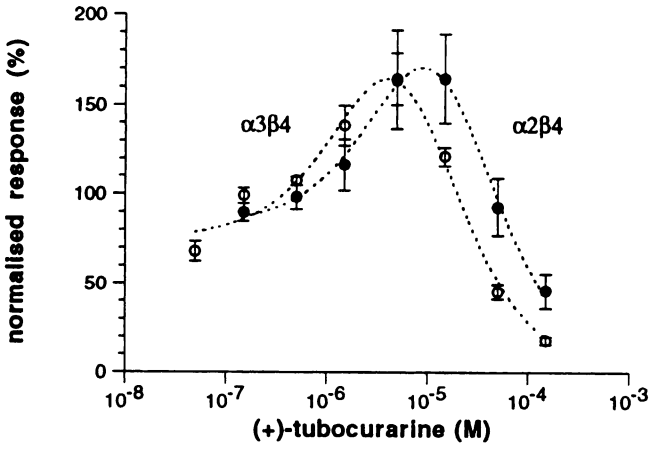

Fig. 5. Enhancement of the peak response to ACh induced by (+)-tubocurarine with α2β4 and α3β4 neuronal nAChRs. Control responses evoked by ACh alone were used to normalize the responses obtained in the presence of (+)-tubocurarine. Each *point* is the mean ± standard error [α2β4, $n = 4$ from two donors (●); α3β4, $n = 5$ from two donors (○)]. The estimates of K_b obtained by fitting eq. 5 (see Materials and Methods) to the data points were 12 ± 0.7 μM (α2β4) and 5.2 ± 0.6 μM (α3β4). The estimates of factor f used to account for the relative contribution of the ABR state with respect to the open state were 0.14 and 0.15 for α2β4 and α3β4 receptors, respectively (see Materials and Methods). The normalized agonist concentration c_A was constrained to 0.04 (with the exact values being 0.05 and 0.03 for α2β4 and α3β4 receptors, respectively).

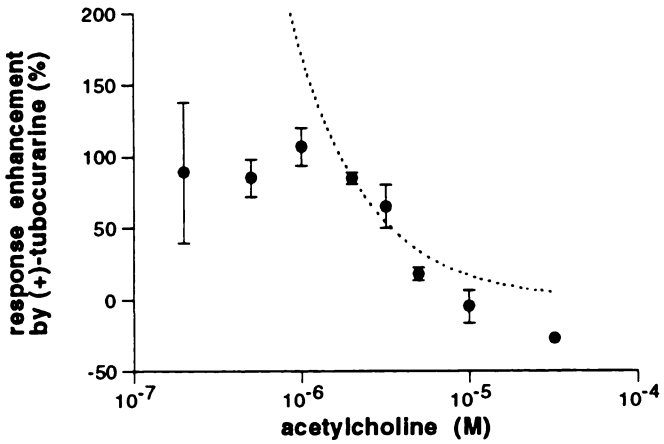

Fig. 6. Normalized responses in the presence of 1.5 μM (+)-tubocurarine and various ACh concentrations with α2β4 neuronal nAChRs. Responses were obtained in $BaCl_2$ medium. For each ACh concentration the response obtained in the presence of 1.5 μM (+)-tubocurarine was normalized with respect to the control response obtained with agonist only, and the enhancement was calculated as 100 × (ratio − 1). Each *point* is the average ± standard error of values obtained in two to six oocytes ($n = 1$ at 32 μM ACh) from one donor. *Dotted line*, calculated ratio $(c_A^2 + 2fc_Ac_B)/c_A^2$, using parameters obtained in this study ($c_A = x_A/44$, $c_B = 1.5/12$, and $f = 0.14$) (see Table 1 and the legend to Fig. 5).

Discussion

Concentration-Response Curves

We have investigated the effect of (+)-tubocurarine on four different rat neuronal nAChR types (α2β2, α2β4, α3β2, and α3β4) expressed in *Xenopus* oocytes. (+)-Tubocurarine inhibited ACh-evoked responses when applied to α2β2 and α3β2 receptors. In contrast, it both enhanced and inhibited agonist-evoked responses with α2β4 and α3β4 receptors. A maximal increase was observed at concentrations around 10 μM. (+)-Tubocurarine alone did not elicit any measurable response. Our results suggest that this unusual effect of (+)-tubocurarine on neuronal nAChRs expressed in *Xenopus* oocytes is linked to the β4 subunit.

Initial work was designed to estimate the apparent equilibrium dissociation constants (K_a) for ACh in each neuronal nAChR type. True equilibrium dissociation constants for ACh (K_d) cannot be determined, because the efficacy of ACh with any of these receptor types is unknown.

The use of nominally calcium-free $BaCl_2$ medium affected the K_a of all subunit combinations. The changes depended on the β subunit incorporated into the receptors; the K_a values were reduced by a factor of 1.8 for α2β2 and α3β2 receptors but increased by factors of 2.3 and 1.5 for α2β4 and α3β4 receptors, respectively (Table 1). The latter observation is consistent with

previously published data showing that external Ca^{2+} directly modulates the activity of $\alpha3\beta4$ receptors (34). Our data now extend this observation to $\alpha2\beta4$ nAChRs. The shift to the left of concentration-response curves for $\beta2$-containing receptors could reflect an opposite negative modulatory effect of external Ca^{2+} on these receptor types.

It is likely that indirect activation of Ca^{2+}-dependent chloride channels causes a significant distortion of the concentration-response curves, particularly at high agonist concentrations. We previously observed a long and shallow left tail and a low Hill coefficient in concentration-response curves for rat $\alpha3\beta2$ nAChRs (17). Such curves could be due to the expression of two (or more) nAChR types with different K_a values and relative contributions to the overall response after injection of a single combination of mRNAs. This phenomenon has already been observed after injection of cloned muscle-type receptor subunits in *Xenopus* oocytes (35). The K_a of rat $\alpha3\beta2$ nAChRs obtained in this study was much lower than the estimate obtained in a previous study of the same receptor type (350 μM) (17). It is still a matter of debate to what extent uncontrolled stoichiometry of mRNAs injected into *Xenopus* oocytes may cause variability in agonist sensitivity (see Ref. 6 for a discussion).

Replacing the $\alpha3$ subunit with $\alpha2$ did not yield a systematic change of K_a values; $\alpha2\beta2$ receptors were less sensitive to ACh than were $\alpha3\beta2$ receptors, whereas $\alpha2\beta4$ receptors were more sensitive to ACh than were $\alpha3\beta4$ receptors. Our results confirm the observation that both α and β subunits determine the agonist sensitivity of neuronal nAChRs (13).

Inhibition Curves

(+)-Tubocurarine effects on $\alpha2\beta2$ and $\alpha3\beta2$ receptors. (+)-Tubocurarine inhibited $\alpha2\beta2$ and $\alpha3\beta2$ neuronal nAChRs. What is the likely mechanism of action of (+)-tubocurarine on these receptors? (+)-Tubocurarine is a competitive antagonist of ACh at chick $\alpha4$/non-α nAChRs (23), as well as neuronal nAChRs of frog cardiac and paravertebral neurons (22). On the other hand, (+)-tubocurarine has been shown to cause noncompetitive forms of antagonism (open channel block) in parasympathetic rat ganglion cells (36). We did not observe signs of open channel block, such as increased rate of current decay during antagonist application when (+)-tubocurarine was coapplied, with $\alpha2\beta2$ or $\alpha3\beta2$ receptors. Neither did we see signs of channel reopening (e.g., brief increase of the response) after removal of the agonist and antagonist solution (Fig. 2). Additional experiments (e.g., using different holding potentials) are required to determine the mechanism of inhibition by (+)-tubocurarine of $\alpha2\beta2$ and $\alpha3\beta2$ nAChRs.

Bell-shaped inhibition curves. The concentration-response curves for $\alpha2\beta4$ and $\alpha3\beta4$ neuronal nAChRs were bell-shaped, thus reflecting a dual action of (+)-tubocurarine on these receptor types. It has been shown that (+)-tubocurarine both opens and blocks nAChRs of bovine chromaffin cells (26). However, because (+)-tubocurarine alone had no effect on $\beta4$-containing receptors, we can exclude a direct partial agonistic effect of (+)-tubocurarine.

We have used a simplified six-state kinetic scheme, in which each of the two binding sites can be independently occupied by either ACh or (+)-tubocurarine molecules, to fit the inhibition curves for $\beta4$-containing receptors (see Materials and Methods). Because the presence of both ACh and (+)-tubocurarine was required to observe an enhancement of the response, we assumed, as a working hypothesis, that the intermediate [ACh- and (+)-tubocurarine-liganded] state ("ABR") is also conducting. The equation linked to this model (eq. 5) yielded a number of predictions, some of which were verified by experimental data.

The concentration-response curve should become bell-shaped, and the estimates of K_b for (+)-tubocurarine obtained by fitting the corresponding equation to the data (Fig. 5) were in the range of concentrations yielding the maximal response increases (see legend to Fig. 5). Applying a more potent agonist should reduce the size of the response enhancement by decreasing the occupancy of the intermediate state. This prediction was verified by the experiments with DMPP (an agonist more potent than ACh) (17), ACh, and nicotine with $\alpha3\beta4$ receptors. Responses evoked by 5 μM DMPP were about 3 times larger than responses elicited by either 20 μM ACh or 30 μM nicotine (see Results) and were not enhanced by coapplication of 1.5 μM (+)-tubocurarine. Also, increasing the agonist concentration in the presence of a constant (+)-tubocurarine concentration should gradually abolish the response enhancement. This was indeed the case when the ACh concentration was raised from 2 to 32 μM (Fig. 6).

Conversely, the absence of enhancement by (+)-tubocurarine with $\beta2$ receptors might be due to the application of an excessive agonist concentration, so that the occupancy of the ABR state would be too low to yield significant response enhancement. However, even at much lower ACh concentrations (320 nM) we failed to detect any enhancement of the ACh-evoked responses by 5 μM (+)-tubocurarine with $\alpha2\beta2$ and $\alpha3\beta2$ receptors (n = 4 for both combinations) (data not shown). These results further confirm the specificity of the $\beta4$ subunit in mediating the effect of (+)-tubocurarine.

On the other hand, we also observed a number of discrepancies between the model and the data. First, we observed a marked inhibition of the ACh-evoked responses by concentrations of (+)-tubocurarine of <1 μM (Fig. 5). These data points (particularly with $\alpha3\beta4$ nAChRs) caused substantial distortion of the estimated control current response I_{max} (by 18% for $\alpha2\beta4$ and 25% for $\alpha3\beta4$). Second, the enhancement of responses evoked by ACh concentrations of <1 μM was about 95%, whereas the model predicted a 10-fold larger enhancement (Fig. 6). Furthermore, the enhancement by (+)-tubocurarine was not simply abolished by increasing agonist concentrations, as expected from a simple competitive antagonism scheme. On the contrary, inhibition by the same (+)-tubocurarine concentration increased with the agonist concentration, suggesting additional noncompetitive antagonism.

Signs of noncompetitive antagonism were indeed observed in individual responses of $\beta4$-containing receptors; these included an increased rate of response decay during application of high antagonist concentrations or reopening of the channel after removal of high antagonist concentrations (Fig. 4). Finally, the responses of all receptor types showed signs of desensitization during agonist application. In conclusion, although our kinetic scheme correctly predicts some of the effects of agonists and (+)-tubocurarine on the peak current, it obviously still requires the incorporation of additional conformational (or functional) states (desensitized, blocked) to better match the experimental data.

We may, finally, ask whether there are physiological corre-

lates to our observations. The observation, made 25 years ago, that coapplication of (+)-tubocurarine potentiated nAChR responses in rat parasympathetic ganglia (36) has remained so far unexplained; the responses to ionophoretically applied carbachol were potentiated by coapplication of 5 μM (+)-tubocurarine, a concentration that caused maximal response increases with α3β4 nAChRs in the present study. Furthermore, the inhibitory action of (+)-tubocurarine was increased when (+)-tubocurarine was coapplied with higher agonist concentrations (36).

Our study suggests that the observation of similar effects of (+)-tubocurarine with native receptors and β4-containing receptors expressed in *Xenopus* oocytes is due to the presence of the β4 subunit in native receptors. We have recently shown that both α3 and β4 genes are indeed widely expressed in the neurons of rat autonomic ganglia and adrenal medulla (37). The (+)-tubocurarine-induced increase of the agonist-evoked response of neuronal nAChRs presented here is, however, much larger than that observed with native receptors. This difference could reflect the use of different experimental protocols. It may also point to structural differences between native and heterogeneously expressed neuronal nAChRs, such as the absence of an α subunit isoform (e.g., α5) in the latter (8, 9). The increase by (+)-tubocurarine of responses elicited by low agonist concentrations may become a useful tool to detect the presence of the β4 subunit in native neuronal nAChRs of unknown subunit composition.

Acknowledgments

cDNA clones were gifts from Drs. J. Boulter and S. Heinemann (The Salk Institute, La Jolla, CA) and Dr. J. Patrick (Baylor College, Houston, TX). We thank Drs. Reuter and Sigel for support and helpful discussions.

References

1. Lingle, C. J., D. Maconochie, and J. H. Steinbach. Activation of skeletal muscle nicotinic acetylcholine receptors. *J. Membr. Biol.* **126**:195–217 (1992).
2. Galzi, J.-L., F. Revah, A. Bessis, and J.-P. Changeux. Functional architecture of the nicotinic acetylcholine receptor: from electric organ to brain. *Annu. Rev. Pharmacol.* **31**:37–72 (1991).
3. Deneris, E. S., J. Connolly, S. W. Rogers, and R. Duvoisin. Pharmacological and functional diversity of neuronal nicotinic acetylcholine receptors. *Trends Pharmacol. Sci.* **12**:34–40 (1991).
4. Role, L. W. Diversity in primary structure and function of neuronal nicotinic acetylcholine receptor channels. *Curr. Opin. Neurobiol.* **2**:254–262 (1992).
5. Sargent, P. B. The diversity of neuronal nicotinic acetylcholine receptors. *Annu. Rev. Neurosci.* **16**:403–443 (1993).
6. Devillers-Thiéry, A., J. L. Galzi, J. L. Eiselé, S. Bertrand, D. Bertrand, and J. P. Changeux. Functional architecture of the nicotinic acetylcholine receptor: a prototype of ligand-gated ion channels. *J. Membr. Biol.* **136**:97–112 (1993).
7. Listerud, M., A. B. Brussard, P. Devay, D. R. Colman, and L. N. Role. Functional contribution of neuronal AChR subunits revealed by antisense oligonucleotides. *Science (Washington D. C.)* **254**:1518–1521 (1991).
8. Vernallis, A. B., W. G. Conroy, and D. K. Berg. Neurons assemble acetylcholine receptors with as many as three kinds of subunits while maintaining subunit segregation among receptor subtypes. *Neuron* **10**:451–464 (1993).
9. Conroy, W. G., A. B. Vernallis, and D. K. Berg. The α5 gene product assembles with multiple acetylcholine receptor subunits to form distinctive receptor subtypes in brain. *Neuron* **9**:679–691 (1992).
10. Colquhoun, D., D. C. Ogden, and A. Mathie. Nicotinic acetylcholine receptors of nerve and muscle: functional aspects. *Trends Pharmacol. Sci.* **8**:465–472 (1987).
11. Wheeler, S. V., J. E. Chad, and R. Foreman. Residues 1 to 80 of the N-terminal domain of the β subunit confer neuronal bungarotoxin sensitivity and agonist selectivity on neuronal nicotinic receptors. *FEBS Lett.* **332**:139–142 (1993).
12. Clarke, P. B. S. The fall and rise of neuronal α-bungarotoxin binding proteins. *Trends Pharmacol. Sci.* **13**:407–413 (1992).
13. Luetje, C. W., and J. Patrick. Both α and β-subunits contribute to the agonist sensitivity of neuronal nicotinic acetylcholine receptors. *J. Neurosci.* **11**:837–845 (1991).
14. Luetje, C. W., M. Piattoni, and J. Patrick. Mapping of ligand binding sites of neuronal nicotinic acetylcholine receptors using chimeric α subunits. *Mol. Pharmacol.* **44**:657–666 (1993).
15. Stafford, G. A., R. E. Oswald, and G. A. Weiland. The β subunit of neuronal nicotinic acetylcholine receptors is a determinant of the affinity for substance P inhibition. *Mol. Pharmacol.* **45**:758–762 (1994).
16. Gross, A., M. Ballivet, D. Rungger, and D. Bertrand. Neuronal nicotinic acetylcholine receptors expressed in *Xenopus* oocytes: role of the α subunit in agonist sensitivity and desensitization. *Pflügers Arch.* **419**:545–551 (1991).
17. Cachelin, A. B., and R. Jaggi. β subunits determine the time course of desensitization in rat α3 neuronal nicotinic acetylcholine receptors. *Pflügers Arch.* **419**:579–582 (1991).
18. Papke, R. L., and S. F. Heinemann. The role of the β4 subunit in determining the kinetic properties of rat neuronal nicotinic acetylcholine α3-receptors. *J. Physiol. (Lond.)* **440**:95–112 (1991).
19. Mulle, C., D. Choquet, H. Korn, and J.-P. Changeux. Calcium influx through nicotinic receptor in rat central neurons: its relevance to cellular regulation. *Neuron* **8**:135–143 (1992).
20. Séguéla, P., J. Wadiche, K. Dineley-Miller, J. A. Dani, and J. W. Patrick. Molecular cloning, functional properties, and distribution of rat brain α7: a nicotinic cation channel highly permeable to calcium. *J. Neurosci.* **13**:596–604 (1993).
21. Colquhoun, D., F. Dreyer, and R. E. Sheridan. The actions of tubocurarine at the frog neuromuscular junction. *J. Physiol. (Lond.)* **293**:247–284 (1979).
22. Lipscombe, D., and H. P. Rang. Nicotinic receptors of frog ganglia resemble pharmacologically those of skeletal muscle. *J. Neurosci.* **8**:3258–3265 (1988).
23. Bertrand, D., M. Ballivet, and D. Rungger. Activation and blocking of neuronal nicotinic acetylcholine receptor reconstituted in *Xenopus* oocytes. *Proc. Natl. Acad. Sci. USA* **87**:1993–1997 (1990).
24. Trautmann, A. Curare can open and block ionic channels associated with cholinergic receptors. *Nature (Lond.)* **298**:272–275 (1982).
25. Sine, S. M., and J. H. Steinbach. Acetylcholine receptor activation by a site-selective ligand: nature of brief open and closed states in BC_3H-1 cells. *J. Physiol. (Lond.)* **370**:357–379 (1986).
26. Nooney, J. M., J. A. Peters, and J. J. Lambert. A patch clamp study of the nicotinic acetylcholine receptor of bovine adrenomedullary chromaffin cells in culture. *J. Physiol. (Lond.)* **455**:503–527 (1992).
27. Krieg, P. A., and D. A. Melton. Functional messenger RNAs are produced by SP6 *in vitro* transcription of cloned cDNAs. *Nucleic Acids Res.* **12**:7057–7070 (1984).
28. Drummond, D. R., J. Armstrong, and A. Colman. The effect of capping and polyadenylation on the stability, movement and translation of synthetic messenger RNAs in *Xenopus* oocytes. *Nucleic Acids Res.* **13**:7375–7394 (1985).
29. Dumont, J. N. Oogenesis in *Xenopus laevis* (Daudin). *J. Morphol.* **136**:153–180 (1972).
30. Sigel, E. Properties of single sodium channels translated by *Xenopus* oocytes after injection with messenger ribonucleic acid. *J. Physiol. (Lond.)* **386**:73–90 (1987).
31. White, M. M., and M. Aylwin. Niflumic and flufenamic acids are potent reversible blockers of Ca^{2+}-activated Cl^- channels in *Xenopus* oocytes. *Mol. Pharmacol.* **37**:720–724 (1990).
32. Craig, D. A. The Cheng-Prusoff relationship: something lost in the translation. *Trends Pharmacol. Sci.* **14**:89–91 (1993).
33. Colquhoun, D., and R. E. Sheridan. The effect of tubocurarine competition on the kinetics of agonist action on the nicotinic receptor. *Br. J. Pharmacol.* **75**:77–86 (1982).
34. Vernino, S., M. Amador, C. W. Luetje, J. Patrick, and J. A. Dani. Calcium modulation and high calcium permeability of neuronal nicotinic acetylcholine receptors. *Neuron* **68**:127–134 (1992).
35. Gibb, A. J., H. Kojima, J. A. Carr, and D. Colquhoun. Expression of cloned receptor subunits produces multiple receptors. *Proc. R. Soc. Lond. B Biol. Sci.* **242**:108–112 (1990).
36. Ascher, P., W. A. Large, and H. P. Rang. Studies on the mechanism of action of acetylcholine antagonists on rat parasympathetic ganglion cells. *J. Physiol. (Lond.)* **295**:139–170 (1979).
37. Rust, G., J.-M. Burgunder, T. E. Lauterburg, and A. B. Cachelin. Expression of neuronal nicotinic acetylcholine receptor subunit genes in the rat autonomic nervous system. *Eur. J. Neurosci.* **6**:478–485 (1994).

Send reprint requests to: Armand B. Cachelin, Department of Pharmacology, University of Berne, Friedbühlstrasse 49, 3010 Bern, Switzerland.